$b \to c\tau\bar{\nu}$ decay in supersymmetry with R-parity violation*

Dong-Yang Wang(王东洋)[1)] Ya-Dong Yang(杨亚东)[2)] Xing-Bo Yuan(袁兴博)[3)]

Institute of Particle Physics and Key Laboratory of Quark and Lepton Physics (MOE),
Central China Normal University, Wuhan 430079, China

Abstract: In past years, several hints of lepton flavor universality (LFU) violation have emerged from the $b \to c\tau\bar{\nu}$ and $b \to s\ell^+\ell^-$ data. More recently, the Belle Collaboration has reported the first measurement of the D^* longitudinal polarization fraction in the $B \to D^*\tau\bar{\nu}$ decay. Motivated by this intriguing result, along with the recent measurements of $R_{J/\psi}$ and τ polarization, we present the study of $b \to c\tau\bar{\nu}$ decays in supersymmetry (SUSY) with R-parity violation (RPV). We consider $B \to D^{(*)}\tau\bar{\nu}$, $B_c \to \eta_c\tau\bar{\nu}$, $B_c \to J/\psi\tau\bar{\nu}$ and $\Lambda_b \to \Lambda_c\tau\bar{\nu}$ modes and focus on the branching ratios, LFU ratios, forward-backward asymmetries, polarizations of daughter hadrons, and the τ lepton. The RPV SUSY was capable of explaining the $R_{D^{(*)}}$ anomalies at the 2σ level, after taking into account various flavor constraints. In the allowed parameter space, the differential branching fractions and LFU ratios are largely enhanced by the SUSY effects, especially in the large dilepton invariant mass region. Moreover, a lower bound $\mathcal{B}(B^+ \to K^+\nu\bar{\nu}) > 7.37\times 10^{-6}$ is obtained. These observables could provide testable signatures at the high-luminosity LHC and SuperKEKB, and correlate with direct searches for SUSY.

Keywords: supersymmetry, R-parity violation, heavy flavor hadron, b-quark semi-leptonic decay

PACS: 13.25.Hw, 13.30.Ce **DOI:** 10.1088/1674-1137/43/8/083103

1 Introduction

In the recent years, several interesting anomalies emerged in the experimental data of semi-leptonic B-meson decays. The ratios $R_{D^{(*)}} \equiv \mathcal{B}(B \to D^{(*)}\tau\bar{\nu})/\mathcal{B}(B \to D^{(*)}\ell\bar{\nu})$ with $\ell = e,\mu$, obtained by latest averages of the measurements by BaBar [1, 2], Belle [3–6] and LHCb Collaboration [7–9], yield [10]

$$\begin{aligned} R_D^{\rm exp} &= 0.407 \pm 0.039\,({\rm stat.}) \pm 0.024\,({\rm syst.}),\\ R_{D^*}^{\rm exp} &= 0.306 \pm 0.013\,({\rm stat.}) \pm 0.007\,({\rm syst.})\,. \end{aligned} \tag{1}$$

In comparison to the branching fractions, these ratios have the advantage that, apart from the significant reduction of the experimental systematic uncertainties, the CKM matrix element V_{cb} cancels out, and the sensitivity to $B \to D^{(*)}$ transition form factors becomes much weaker. The SM predictions read [10]

$$R_D^{\rm SM} = 0.299 \pm 0.003, \qquad R_{D^*}^{\rm SM} = 0.258 \pm 0.005, \tag{2}$$

which are obtained from the arithmetic averages of the most recent calculations performed by several groups [11-14]. The SM predictions for R_D and R_{D^*} have values below the experimental measurements by 2.3σ and 3.0σ, respectively. Taking into account the measurement correlation of -0.203 between R_D and R_{D^*}, the combined experimental results exhibit about 3.78σ deviation from the SM predictions [10]. For the $B_c \to J/\psi\tau\bar{\nu}$ decay, which is mediated by the same quark-level process as $B \to D^{(*)}\tau\bar{\nu}$, the recently measured ratio $R_{J/\psi}^{\rm exp} = 0.71 \pm 0.17\,({\rm stat.}) \pm 0.18\,({\rm syst.})$ at the LHCb [15] lies within about 2σ above the SM prediction $R_{J/\psi}^{\rm SM} = 0.248 \pm 0.006$ [16]. In addition, the LHCb measurements of the ratios $R_{K^{(*)}} \equiv \mathcal{B}(B \to K^{(*)}\mu^+\mu^-)/\mathcal{B}(B \to K^{(*)}e^+e^-)$, $R_K^{\rm exp} = 0.745^{+0.090}_{-0.074} \pm 0.036$ for $q^2 \in [1.0, 6.0]\,{\rm GeV}^2$ [17] and $R_{K^*}^{\rm exp} = 0.69^{+0.11}_{-0.07} \pm 0.05$ for $q^2 \in [1.1, 6.0]\,{\rm GeV}^2$ [18], are found to be about 2.6σ and 2.5σ lower than the SM expectation, $R_{K^{(*)}}^{\rm SM} \simeq 1$ [19, 20], respectively. These measurements, referred to as the $R_{D^{(*)}}$,

Received 11 April 2019, Published online 17 June 2019

* Supported by the National Natural Science Foundation of China (11775092, 11521064, 11435003, 11805077), XY is also supported in part by the startup research funding from CCNU

1) E-mail: wangdongyang@mails.ccnu.edu.cn
2) E-mail: yangyd@mail.ccnu.edu.cn
3) E-mail: y@mail.ccnu.edu.cn

$R_{J/\psi}$, and $R_{K^{(*)}}$ anomalies, may provide hints of the Lepton Flavor University (LFU) violation and have motivated numerous studies of new-physics (NP) both in the effective field theory (EFT) approach [21–34] and in specific NP models [35–60]. We refer to Refs. [61, 62] for recent reviews.

The first measurement on the D^* longitudinal polarization fraction in the $B \to D^* \tau \bar{\nu}$ decay has recently been reported by the Belle Collaboration [63, 64]

$$P_L^{D^*} = 0.60 \pm 0.08\,(\text{stat.}) \pm 0.04\,(\text{syst.}),$$

which is consistent with the SM prediction of $P_L^{D^*} = 0.46 \pm 0.04$ [65] at 1.5σ. Previously, the Belle Collaboration also performed measurements on τ polarization in the $B \to D^* \tau \bar{\nu}$ decay and obtained the result $P_L^{\tau} = -0.38 \pm 0.51\,(\text{stat.})^{+0.21}_{-0.16}\,(\text{syst.})$ [5, 6]. Angular distributions can provide valuable information about the spin structure of the interaction in $B \to D^{(*)} \tau \bar{\nu}$ decays, and they are good observables for the testing of various NP explanations [66–70]. Measurements of angular distributions are expected to significantly improve in the future. For example, Belle II with $50\,\text{ab}^{-1}$ data can measure P_L^{τ} with a precision of ± 0.07 [71].

In this work, motivated by these recent experimental progresses, we study the $R_{D^{(*)}}$ anomalies in the supersymmetry (SUSY) with R-parity violation (RPV). In this scenario, the down-type squarks interact with quarks and leptons via RPV couplings. Therefore, they contribute to the $b \to c \tau \bar{\nu}$ transition at the tree level and could explain the current $R_{D^{(*)}}$ anomalies [72–74]. Besides $B \to D^{(*)} \tau \bar{\nu}$, we will also study the $B_c \to J/\psi \tau \bar{\nu}$, $B_c \to \eta_c \tau \bar{\nu}$, and $\Lambda_b \to \Lambda_c \tau \bar{\nu}$ decay. All of them depict the $b \to c \tau \bar{\nu}$ transition at the quark level, whereas the latter two decays have not been measured yet. Using the latest experimental data of various low-energy flavor processes, we derive the constraints of the RPV couplings. Subsequently, predictions in the RPV SUSY are made for the five $b \to c \tau \bar{\nu}$ decays, focusing on the q^2 distributions of the branching fractions, LFU ratios, and various angular observables. We have also taken into account recent developments regarding the form factors [11, 14, 16, 75, 76]. Implications for future research at the high-luminosity LHC (HL-LHC) and SuperKEKB are briefly discussed.

This paper is organized as follows: in Section 2, we briefly review the SUSY with RPV interactions. In Section 3, we recapitulate the theoretical formulae for various flavor processes, and discuss the SUSY effects. In Section 4, detailed numerical results and discussions are presented. We present the conclusions in Section 5. The relevant form factors are recapitulated in Appendix A.

2 Supersymmetry with *R*-parity violation

The most general re-normalizable RPV terms in the superpotential are given by [77, 78]

$$\begin{aligned} W_{\text{RPV}} =& \mu_i L_i H_u + \frac{1}{2}\lambda_{ijk} L_i L_j E_k^c + \lambda'_{ijk} L_i Q_j D_k^c \\ &+ \frac{1}{2}\lambda''_{ijk} U_i^c D_j^c D_k^c, \end{aligned} \tag{3}$$

where L and Q denote the $SU(2)$ doublet lepton and quark superfields, respectively. E and U (D) depict the singlet lepton and quark superfields, respectively. i, j and k indicate generation indices. To ensure the proton stability, we assume the couplings λ''_{ijk} are zero. In semi-leptonic B meson decays, contribution from the λ term occurs through the exchange of sleptons, and it is much more suppressed than the one from the λ' term, which occurs through the exchange of right-handed down-type squarks [72]. Therefore, we only consider the $\lambda'_{ijk} L_i Q_j D_k^c$ term in this work. For the SUSY scenario with the λ term, studies on the $R_{D^{(*)}}$ anomalies with slepton exchanges can be found in Refs. [79, 80].

The interaction with λ'_{ijk} couplings can be expanded in terms of fermions and sfermions as [72]

$$\begin{aligned} \Delta\mathcal{L}_{\text{RPV}} =& -\lambda'_{ijk}\Big[\tilde{\nu}_L^i \bar{d}_R^k d_L^j + \tilde{d}_L^j \bar{d}_R^k \nu_L^i + \tilde{d}_R^{k*} \bar{\nu}_R^{ci} d_L^j \\ &- V_{jl}(\tilde{\ell}_L^i \bar{d}_R^k u_L^l + \tilde{u}_L^l \bar{d}_R^k \ell_L^i + \tilde{d}_R^{k*} \bar{\ell}_R^{ci} u_L^l)\Big] + \text{h.c.}, \end{aligned} \tag{4}$$

where V_{ij} denotes the CKM matrix element. Here, all the SM fermions $d_{L,R}$, $\ell_{L,R}$, and ν_L are in their mass eigenstate. Since we neglect the tiny neutrino masses, the PMNS matrix is not needed for the lepton sector. For the sfermions, we assume that they are in the mass eigenstate. We refer to Ref. [77] for more details about the choice of basis. Finally, we adopt the assumption in Ref. [74] stating that only the third family is effectively supersymmetrized. This case is equivalent to the one where the first two generations are decoupled from the low-energy spectrum, as in Refs. [81, 82]. For the studies including the first two generation sfermions, we refer to Ref. [73], where both the $R_{D^{(*)}}$ and $R_{K^{(*)}}$ anomalies are discussed.

The down-type squarks and the scalar leptoquark (LQ) discussed in Ref. [83] have similar interactions with the SM fermions. However, in the most general case, the LQ can couple to the right-handed $SU(2)_L$ singlets, which is forbidden in the RPV SUSY. Such right-handed couplings are important to explain the $(g-2)_\mu$ anomaly in the LQ scenario [83]. Moreover, these couplings can also affect semi-leptonic B decays. In particular, their contributions to the $B \to D^{(*)} \tau \bar{\nu}$ decays are found to be small after considering other flavor constraints [52].

3 Observables

In this section, we introduce the theoretical framework of the relevant flavor processes and discuss the RPV SUSY effects in these processes.

3.1 $b \to c(u)\tau\bar{\nu}$ transitions

With the RPV SUSY contributions, the effective Hamiltonian responsible for $b \to c(u)\tau\bar{\nu}_\tau$ transitions is given by [72]

$$\mathcal{H}_{\rm eff} = \frac{4G_{\rm F}}{\sqrt{2}} \sum_{i=u,c} V_{ib}(1+C^{\rm NP}_{L,i})(\bar{u}_i\gamma^\mu P_L b)(\bar{\tau}\gamma_\mu P_L \nu_\tau), \quad (5)$$

where tree-level sbottom exchange yields

$$C^{\rm NP}_{L,i} = \frac{v^2}{4m^2_{\tilde{b}_R}} \lambda'_{333} \sum_{j=1}^{3} \lambda'^*_{3j3} \left(\frac{V_{ij}}{V_{i3}}\right), \quad (6)$$

with the Higgs vev $v = 246$ GeV. This Wilson coefficient is at the matching scale $\mu_{\rm NP} \sim m_{\tilde{b}_R}$. However, since the corresponding current is conserved, we can obtain the low-energy Wilson coefficient without considering the renormalization group evolution (RGE) effects, i.e., $C^{\rm NP}_{L,i}(\mu_b) = C^{\rm NP}_{L,i}(\mu_{\rm NP})$.

For $b \to c\ell\bar{\nu}$ transitions, we consider five processes, including $B \to D^{(*)}\ell\bar{\nu}$ [84-86], $B_c \to \eta_c\ell\bar{\nu}$ [16, 87], $B_c \to J/\psi\ell\bar{\nu}$ [88–96], and $\Lambda_b \to \Lambda_c\ell\bar{\nu}$ [97-100] decays. All these decays can be uniformly denoted as

$$M(p_M,\lambda_M) \to N(p_N,\lambda_N) + \ell^-(p_\ell,\lambda_\ell) + \bar{\nu}_\ell(p_{\bar{\nu}_\ell}), \quad (7)$$

where $(M,N) = (B,D),(B_c,\eta_c),(B,D^*),(B_c,J/\psi)$, and (Λ_b,Λ_c), and $(\ell,\bar{\nu}) = (e,\bar{\nu}_e),(\mu,\bar{\nu}_\mu)$, and $(\tau,\bar{\nu}_\tau)$. For each particle i in the above decay, its momentum and helicity are denoted as p_i and λ_i, respectively. In particular, the helicity of pseudoscalar meson is zero, e.g., $\lambda_D = 0$. After summation of the helicity of parent hadron M, the differential decay width for this process can be written as [67, 101]

$$\mathrm{d}\Gamma^{\lambda_N,\lambda_\ell}(M \to N\ell^-\bar{\nu}_\ell) = \frac{1}{1+2|\lambda_M|} \sum_{\lambda_M} \left|\mathcal{M}^{\lambda_M}_{\lambda_N,\lambda_\ell}\right|^2 \frac{\sqrt{Q_+Q_-}}{512\pi^3 m_M^3} \times \sqrt{1-\frac{m^2_\ell}{q^2}}\,\mathrm{d}q^2\,\mathrm{d}\cos\theta_\ell, \quad (8)$$

where $q = p_M - p_N$, $m_\pm = m_M \pm m_N$, and $Q_\pm = m^2_\pm - q^2$. The angle $\theta_\ell \in [0,\pi]$ denotes the angle between the three-momentum of ℓ and that of N in the ℓ-$\bar{\nu}$ center-of-mass frame. The following observables can be derived with the differential decay width:

• The decay width and branching ratio

$$\frac{\mathrm{d}\mathcal{B}}{\mathrm{d}q^2} = \frac{1}{\Gamma_M}\frac{\mathrm{d}\Gamma}{\mathrm{d}q^2} = \frac{1}{\Gamma_M}\sum_{\lambda_N,\lambda_\ell}\frac{\mathrm{d}\Gamma^{\lambda_N,\lambda_\ell}}{\mathrm{d}q^2}, \quad (9)$$

where Γ_M is the total width of the hadron M.

• The LFU ratio

$$R_N(q^2) = \frac{\mathrm{d}\Gamma(M \to N\tau\bar{\nu}_\tau)/\mathrm{d}q^2}{\mathrm{d}\Gamma(M \to N\ell\bar{\nu}_\ell)/\mathrm{d}q^2}, \quad (10)$$

where $\mathrm{d}\Gamma(M \to N\ell\bar{\nu}_\ell)/\mathrm{d}q^2$ in the denominator denotes the average of different decay widths of the electronic and muonic modes.

• The lepton forward-backward asymmetry

$$A_{\rm FB}(q^2) = \frac{\int_0^1 \mathrm{d}\cos\theta_\ell(\mathrm{d}^2\Gamma/\mathrm{d}q^2\mathrm{d}\cos\theta_\ell) - \int_{-1}^0 \mathrm{d}\cos\theta_\ell(\mathrm{d}^2\Gamma/\mathrm{d}q^2\mathrm{d}\cos\theta_\ell)}{\mathrm{d}\Gamma/\mathrm{d}q^2}. \quad (11)$$

• The polarization fractions

$$P^\tau_L(q^2) = \frac{\mathrm{d}\Gamma^{\lambda_\tau=+1/2}/\mathrm{d}q^2 - \mathrm{d}\Gamma^{\lambda_\tau=-1/2}/\mathrm{d}q^2}{\mathrm{d}\Gamma/\mathrm{d}q^2},$$
$$P^N_L(q^2) = \frac{\mathrm{d}\Gamma^{\lambda_N=+1/2}/\mathrm{d}q^2 - \mathrm{d}\Gamma^{\lambda_N=-1/2}/\mathrm{d}q^2}{\mathrm{d}\Gamma/\mathrm{d}q^2}, \quad (\text{for } N = \Lambda_c)$$
$$P^N_L(q^2) = \frac{\mathrm{d}\Gamma^{\lambda_N=0}/\mathrm{d}q^2}{\mathrm{d}\Gamma/\mathrm{d}q^2}, \quad (\text{for } N = D^*, J/\psi) \quad (12)$$

Explicit expressions of the helicity amplitudes $\mathcal{M}^{\lambda_M}_{\lambda_N,\lambda_\ell} \equiv \langle N\ell\bar{\nu}_\ell|\mathcal{H}_{\rm eff}|M\rangle$ and all the above observables can be found in Ref. [102] for $B \to D^{(*)}\tau\bar{\nu}$ decays, and Ref. [76] for the $\Lambda_b \to \Lambda_c\tau\bar{\nu}$ decay. The expressions for $B_c \to \eta_c\tau\bar{\nu}$ and $B_c \to J/\psi\tau\bar{\nu}$ are analogical to the ones for $B \to D\tau\bar{\nu}$ and $B \to D^*\tau\bar{\nu}$, respectively. Since these angular observables are ratios of decay widths, they are largely free of hadronic uncertainties, and thus provide excellent tests of lepton flavor universality. The RPV SUSY effects generate the operator with the same chirality structure as in the SM, as shown in Eq. (5). Derivation of the following relation in all the $b \to c\tau\bar{\nu}$ decays is straightforward:

$$\frac{R_N}{R^{\rm SM}_N} = \left|1 + C^{\rm NP}_{L,2}\right|^2, \quad (13)$$

for $N = D^{(*)},\eta_c,J/\psi$, and Λ_c. Here, vanishing contributions to the electronic and muonic channels are assumed.

The hadronic $M \to N$ transition form factors are important inputs to calculate the observables introduced above. In recent years, notable progress has been achieved in this field [11-14, 75, 76, 87, 97, 103–110]. For $B \to D^{(*)}$ transitions, it was already emphasized that the Caprini-Lellouch-Neubert (CLN) parameterization [111] does not account for uncertainties in the values of the subleading Isgur-Wise functions at zero recoil obtained with QCD sum rules [112–114], where the number of parameters is minimal [13]. In this work, we don't use such simplified parameterization, but adopt the conservative approach in Refs. [11, 14], based on the Boyd-Grinstein-Lebed (BGL) parameterization [115]. Furthermore, we use the $B_c \to \eta_c, J/\psi$ transition form factors obtained in the covariant light-front approach [16]. For the $\Lambda_b \to \Lambda_c$ transition form factor, we adopt the recent lattice QCD results from Refs. [75, 76]. Explicit expressions of all the form factors used in our work are recapitulated in Appendix A.

For $b \to u\tau\bar{\nu}$ transitions, we consider $B \to \tau\bar{\nu}$, $B \to \pi\tau\bar{\nu}$ and $B \to \rho\tau\bar{\nu}$ decays. Similar to Eq. (13), we have

$$\frac{\mathcal{B}(B\to\tau\bar{\nu})}{\mathcal{B}(B\to\tau\bar{\nu})_{\rm SM}}=\frac{\mathcal{B}(B\to\pi\tau\bar{\nu})}{\mathcal{B}(B\to\pi\tau\bar{\nu})_{\rm SM}}=\frac{\mathcal{B}(B\to\rho\tau\bar{\nu})}{\mathcal{B}(B\to\rho\tau\bar{\nu})_{\rm SM}}=\left|1+C_{L,1}^{\rm NP}\right|^2. \tag{14}$$

The SUSY contributions to both $b\to u\tau\bar{\nu}$ and $b\to c\tau\bar{\nu}$ transitions depend on the same set of parameters, λ'_{313}, λ'_{323}, and λ'_{333}. Therefore, the ratios $R_{D^{(*)}}$ are related to the $B\to\tau\bar{\nu}$ decay.

3.2 Other processes

The Flavor-Changing Neutral Current (FCNC) decays $B^+\to K^+\nu\bar{\nu}$ and $B^+\to\pi^+\nu\bar{\nu}$ are induced by the $b\to s\nu\bar{\nu}$ and $b\to d\nu\bar{\nu}$ transitions, respectively. In the SM, they are forbidden at the tree level and highly suppressed at the one-loop level due to the GIM mechanism. In the RPV SUSY, the sbottoms can contribute to these decays at the tree level, which results in strong constraints on the RPV couplings. Similar to the $b\to c(u)\tau\bar{\nu}$ transitions, the RPV interactions do not generate new operators beyond the ones presented in the SM. Therefore, we have [73, 74]

$$\begin{aligned}\frac{\mathcal{B}(B^+\to K^+\nu\bar{\nu})}{\mathcal{B}(B^+\to K^+\nu\bar{\nu})_{\rm SM}}&=\frac{2}{3}+\frac{1}{3}\left|1-\frac{v^2}{2m^2_{\tilde{b}_R}}\frac{\pi s_W^2}{\alpha_{\rm em}}\frac{\lambda'_{333}\lambda'^*_{323}}{V_{tb}V^*_{ts}}\frac{1}{X_t}\right|^2,\\ \frac{\mathcal{B}(B^+\to \pi^+\nu\bar{\nu})}{\mathcal{B}(B^+\to \pi^+\nu\bar{\nu})_{\rm SM}}&=\frac{2}{3}+\frac{1}{3}\left|1-\frac{v^2}{2m^2_{\tilde{b}_R}}\frac{\pi s_W^2}{\alpha_{\rm em}}\frac{\lambda'_{333}\lambda'^*_{313}}{V_{tb}V^*_{td}}\frac{1}{X_t}\right|^2,\end{aligned} \tag{15}$$

where the gauge-invariant function $X_t=1.469\pm0.017$ arises from the box and Z-penguin diagrams in the SM [116].

The leptonic W and Z couplings are also important to probe the RPV SUSY effects [26, 117]. In particular, W and Z couplings involving left-handed τ leptons can receive contributions from the loop diagrams mediated by top quark and sbottom. These effects modify the leptonic W and Z couplings as [74]

$$\begin{aligned}\frac{g_{Z\tau_L\tau_L}}{g_{Z\ell_L\ell_L}}&=1-\frac{3|\lambda'_{333}|^2}{16\pi^2}\frac{1}{1-2s_W^2}\frac{m_t^2}{m^2_{\tilde{b}_R}}f_Z\left(\frac{m_t^2}{m^2_{\tilde{b}_R}}\right),\\ \frac{g_{W\tau_L\nu_\tau}}{g_{W\ell_L\nu_\ell}}&=1-\frac{3|\lambda'_{333}|^2}{16\pi^2}\frac{1}{4}\frac{m_t^2}{m^2_{\tilde{b}_R}}f_W\left(\frac{m_t^2}{m^2_{\tilde{b}_R}}\right),\end{aligned} \tag{16}$$

where $\ell=e,\mu$ and $s_W=\sin\theta_W$ with θ_W the weak mixing angle. The loop functions $f_Z(x)$ and $f_W(x)$ have been calculated in Refs. [26, 74, 117] and are given by $f_Z(x)=1/(x-1)-\log x/(x-1)^2$ and $f_W(x)=1/(x-1)-(2-x)\log x/(x-1)^2$. Experimental measurements on the $Z\tau_L\tau_L$ couplings have been performed at the LEP and SLD [118]. Their combined results yield $g_{Z\tau_L\tau_L}/g_{Z\ell_L\ell_L}=1.0013\pm0.0019$ [74]. The $W\tau_L\nu_\tau$ coupling can be extracted from τ decay data. The measured τ decay fractions compared to the μ decay fractions yield $g_{W\tau_L\nu_\tau}/g_{W\ell_L\nu_\ell}=1.0007\pm0.0013$ [74]. Both the leptonic W and Z couplings are measured at the few permille level. Therefore, they assert strong bounds on the RPV coupling λ'_{333}.

RPV interactions can likewise affect K-meson decays, e.g., $K\to\pi\nu\bar{\nu}$, D-meson decays, e.g., $D\to\tau\bar{\nu}$, and τ lepton decays, e.g., $\tau\to\pi\nu$. However, as discussed in Ref. [74], their constraints are weaker than the ones from the processes discussed above. Moreover, the bound from the B_c lifetime [119, 120] is not relevant, since the RPV SUSY contributions to $B_c\to\tau\bar{\nu}$ are not chirally enhanced compared to the SM.

Other interesting anomalies arose in the recent LHCb measurements of $R_{K^{(*)}}\equiv\mathcal{B}(B\to K^{(*)}\mu^+\mu^-)/\mathcal{B}(B\to K^{(*)}e^+e^-)$, which exhibit about 2σ deviation from the SM prediction [17, 18] and are refered to as $R_{K^{(*)}}$ anomalies. The $R_{K^{(*)}}$ anomalies imply hints of LFU violation in $b\to s\ell^+\ell^-$ transition. In the RPV SUSY, the left-handed stop can affect this process at the tree level, and the right-handed sbottom can contribute at the one-loop level. However, as discussed in Ref. [73], once all other flavor constraints are taken into account, no parameter space in the RPV SUSY can explain the current $R_{K^{(*)}}$ anomaly.

Finally, we briefly comment on the direct searches for sbottoms at the LHC. Using data corresponding to 35.9 fb^{-1} at 13 TeV, the CMS collaboration has performed search for heavy scalar leptoquarks in the $pp\to t\bar{t}\tau^+\tau^-$ channel. The results can be directly re-interpreted in the context of pair-produced sbottoms decaying into top quark and τ lepton pairs via the RPV coupling λ'_{333}. Then, the mass of the sbottom is excluded up to 810 GeV at 95% CL [121].

4 Numerical results and discussions

In this section, we proceed to present our numerical analysis for the RPV SUSY scenario introduced in Section 2. We derive the constraints of the RPV couplings and study their effects on various processes.

The most relevant input parameters used in our numerical analysis are presented in Table 1. Employing the theoretical framework described in Section 3, the SM predictions for the $B\to D^{(*)}\tau\bar{\nu}$, $B_c\to\eta_c\tau\bar{\nu}$, $B_c\to J/\psi\tau\bar{\nu}$, and $\Lambda_b\to\Lambda_c\tau\bar{\nu}$ decays are given in Table 2. To obtain the the-

Table 1. Input parameters used in our numerical analysis.

input	value	unit	Ref.
$m_t^{\rm pole}$	173.1 ± 0.9	GeV	[122]
$m_b(m_b)$	4.18 ± 0.03	GeV	[122]
$m_c(m_c)$	1.28 ± 0.03	GeV	[122]
A	$0.8396^{+0.0080}_{-0.0298}$		[123]
λ	$0.224756^{+0.000163}_{-0.000065}$		[123]
$\bar{\rho}$	$0.123^{+0.023}_{-0.023}$		[123]
$\bar{\eta}$	$0.375^{+0.022}_{-0.017}$		[123]

Table 2. Predictions for branching fractions and ratios R of five $b \to c\tau\bar{\nu}$ channels in SM and RPV SUSY. The sign "–" denotes no available measurements at present. Upper limits are all at 90% CL.

observable	unit	SM	RPV SUSY	exp.
$\mathcal{B}(B \to \tau\bar{\nu})$	10^{-4}	$0.947^{+0.182}_{-0.182}$	[0.760, 1.546]	1.44 ± 0.31 [10]
$\mathcal{B}(B^+ \to \pi^+\nu\bar{\nu})$	10^{-6}	$0.146^{+0.014}_{-0.014}$	[0.091, 14.00]	<14 [122]
$\mathcal{B}(B^+ \to K^+\nu\bar{\nu})$	10^{-6}	$3.980^{+0.470}_{-0.470}$	[6.900, 16.00]	<16 [122]
$\mathcal{B}(B \to D\tau\bar{\nu})$	10^{-2}	$0.761^{+0.021}_{-0.055}$	[0.741, 0.847]	0.90 ± 0.24 [122]
R_D		$0.300^{+0.003}_{-0.003}$	[0.314, 0.330]	$0.407 \pm 0.039 \pm 0.024$ [10]
$\mathcal{B}(B_c \to \eta_c\tau\bar{\nu})$	10^{-2}	$0.219^{+0.023}_{-0.029}$	[0.199, 0.262]	–
R_{η_c}		$0.280^{+0.036}_{-0.031}$	[0.262, 0.342]	–
$\mathcal{B}(B \to D^*\tau\bar{\nu})$	10^{-2}	$1.331^{+0.103}_{-0.122}$	[1.270, 1.554]	1.78 ± 0.16 [122]
R_{D^*}		$0.260^{+0.008}_{-0.008}$	[0.267, 0.291]	$0.306 \pm 0.013 \pm 0.007$ [10]
P_L^τ		$-0.467^{+0.067}_{-0.061}$	[−0.528, −0.400]	$-0.38 \pm 0.51^{+0.21}_{-0.16}$ [5, 6]
$P_L^{D^*}$		$0.413^{+0.032}_{-0.031}$	[0.382, 0.445]	$0.60 \pm 0.08 \pm 0.04$ [63, 64]
$\mathcal{B}(B_c \to J/\psi\tau\bar{\nu})$	10^{-2}	$0.426^{+0.046}_{-0.058}$	[0.387, 0.512]	–
$R_{J/\psi}$		$0.248^{+0.006}_{-0.006}$	[0.254, 0.275]	$0.71 \pm 0.17 \pm 0.18$ [15]
$\mathcal{B}(\Lambda_b \to \Lambda_c\tau\bar{\nu})$	10^{-2}	$1.886^{+0.107}_{-0.165}$	[1.807, 2.159]	–
R_{Λ_c}		$0.332^{+0.011}_{-0.011}$	[0.337, 0.372]	–

oretical uncertainties, we vary each input parameter within its 1σ range and add each individual uncertainty in quadrature. For the uncertainties induced by form factors, we also include the correlations among the fit parameters. In particular, for the $\Lambda_b \to \Lambda_c\tau\bar{\nu}$ decay, we follow the treatment of Ref. [75] to obtain the statistical and systematic uncertainties induced by the form factors. From Table 2, we can see that the experimental data on the ratios R_D, R_{D^*} and $R_{J/\psi}$ deviate from the SM predictions by 2.33σ, 2.74σ and 1.87σ, respectively.

4.1 Constraints

In the RPV SUSY scenario introduced in Section 2, the relevant parameters used to explain the $R_{D^{(*)}}$ anomalies are $(\lambda'_{313}, \lambda'_{323}, \lambda'_{333})$ and $m_{\tilde{b}_R}$. In Section 3, we know only that the three products of the RPV couplings, $(\lambda'_{313}\lambda'^*_{333}, \lambda'_{323}\lambda'^*_{333}, \lambda'_{333}\lambda'^*_{333})$, appear in the various flavor processes. In the following analysis, we will assume that these products are real and derive bounds on them. We impose the experimental constraints in the same manner as in Refs. [124, 125], i.e., for each point in the parameter space, if the difference between the corresponding theoretical prediction and experimental data is less than the 2σ (3σ) error bar, which is evaluated by adding the theoretical and experimental errors in quadrature, this point is regarded as allowed at the 2σ (3σ) level. From Section 3, it is known that the RPV couplings always appear in the form of $\lambda'_{3i3}\lambda'^*_{333}/m^2_{\tilde{b}_R}$ in all B decays. Therefore, we can assume $m_{\tilde{b}_R} = 1\,\text{TeV}$ without loss of generality, which is equivalent to absorbing $m_{\tilde{b}_R}$ into $\lambda'_{3i3}\lambda'^*_{333}$. Furthermore, the choice of $m_{\tilde{b}_R} = 1\,\text{TeV}$ is compatible with the direct searches for the sbottoms at CMS [121]. In the SUSY contributions to the couplings $g_{Z\tau_L\tau_L}$ and $g_{W\tau_L\nu_\tau}$ in Eq. (16), additional $m_{\tilde{b}_R}$ dependence arises in the loop functions $f_Z(m_t^2/m^2_{\tilde{b}_R})$ and $f_W(m_t^2/m^2_{\tilde{b}_R})$, respectively. As described in the next subsection, our numerical results show that such $m_{\tilde{b}_R}$ dependence is weak, and the choice of $m_{\tilde{b}_R} = 1\,\text{TeV}$ does not lose much generality.

As shown in Table 2, the current experimental upper bounds imposed on the branching ratio of $B^+ \to K^+\nu\bar{\nu}$ and $B^+ \to \pi^+\nu\bar{\nu}$ are one order above their SM values. However, since the SUSY contributes to these decays at the tree level, the RPV couplings are strongly constrained as

$$\begin{aligned} -0.082 < \lambda'_{313}\lambda'^*_{333} < 0.090, \quad (\text{from} \quad B^+ \to \pi^+\nu\bar{\nu}) \\ -0.098 < \lambda'_{323}\lambda'^*_{333} < 0.057, \quad (\text{from} \quad B^+ \to K^+\nu\bar{\nu}) \end{aligned} \tag{17}$$

at 2σ level. For the leptonic W and Z couplings, the current measurements on $g_{W\tau_L\nu_\tau}/g_{W\ell_L\nu_\ell}$ and $g_{Z\tau_L\tau_L}/g_{Z\ell_L\ell_L}$ have achieved the precision level of a few permille. We find that the latter can yield a stronger constraint, which reads

$$\lambda'_{333}\lambda'^*_{333} < 0.93, \quad (\text{from} \quad g_{Z\tau_L\tau_L}/g_{Z\ell_L\ell_L}) \tag{18}$$

or $|\lambda'_{333}| < 0.96$, at the 2σ level. This upper bound prevents the coupling λ'_{333} from developing a Landau pole below the GUT scale [126].

As discussed in Section 3, the RPV interactions affect $b \to c\tau\bar{\nu}$ transitions via the three products $(\lambda'_{313}\lambda'^*_{333}, \lambda'_{323}\lambda'^*_{333}, \lambda'_{333}\lambda'^*_{333})$. After considering the above individual constraints at 2σ level, the parameter space to explain the current measurements on $R_{D^{(*)}}$, $R_{J/\psi}$, $P_L^\tau(D^*)$ and $P_L^{D^*}$ is shown in Fig. 1 for $m_{\tilde{b}_R} = 1\,\text{TeV}$. The $B \to D^{(*)}\tau\bar{\nu}$ de-

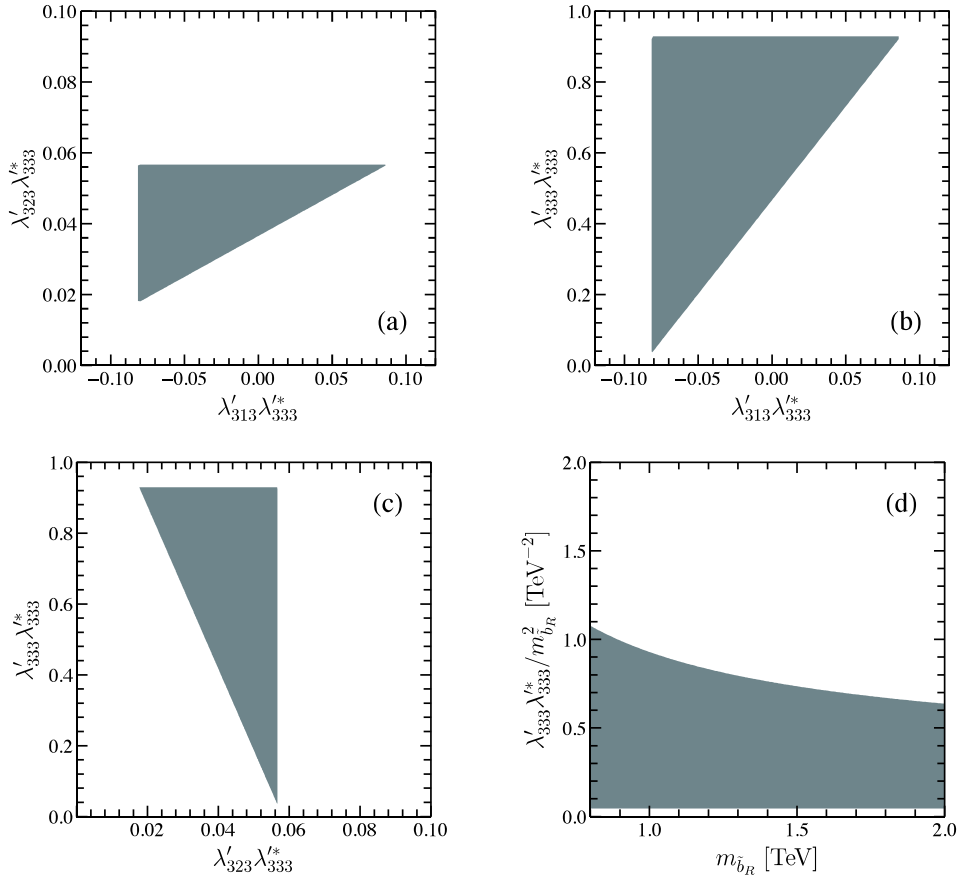

Fig. 1. (color online) Allowed parameter space of $(\lambda'_{313}\lambda'^{*}_{333}, \lambda'_{323}\lambda'^{*}_{333}, \lambda'_{333}\lambda'^{*}_{333})$ by all flavor processes at 2σ level with $m_{\tilde{b}_R} = 1$ TeV, plotted in the $(\lambda'_{313}\lambda'^{*}_{333}, \lambda'_{323}\lambda'^{*}_{333})$ (a), $(\lambda'_{313}\lambda'^{*}_{333}, \lambda'_{333}\lambda'^{*}_{333})$ (b), and $(\lambda'_{323}\lambda'^{*}_{333}, \lambda'_{333}\lambda'^{*}_{333})$ (c) plane. Figure (d) shows the allowed region in $(m_{\tilde{b}_R}, \lambda'_{333}\lambda'^{*}_{333}/m^2_{\tilde{b}_R})$ plane.

cays and other flavor observables are observed to put very stringent constraints on the RPV couplings. The combined constraints are slightly stronger than the individual ones in Eqs. (17) and (18). Moreover, after taking into account the bounds from $B^+ \to K^+\nu\bar{\nu}$ and $g_{Z\tau_L\tau_L}$, the $B \to D^{(*)}\tau\bar{\nu}$ decays are very sensitive to the product $\lambda'_{323}\lambda'^{*}_{333}$. Consequently, current $R_{D^{(*)}}$ anomalies yield a lower bound on $|\lambda'_{323}\lambda'^{*}_{333}|$. Finally, the combined bounds in Fig. 1 read numerically,

$$\begin{aligned} &-0.082 < \lambda'_{313}\lambda'^{*}_{333} < 0.087, \quad \text{(from combined constraints)} \\ &0.018 < \lambda'_{323}\lambda'^{*}_{333} < 0.057, \\ &0.033 < \lambda'_{333}\lambda'^{*}_{333} < 0.928. \end{aligned} \tag{19}$$

As shown, a weak lower bound on $\lambda'_{333}\lambda'^{*}_{333}$ is also obtained. Although the constraints from the D^* polarization fraction $P_L^{D^*}$ are much stronger than the ones from the τ polarization fraction P_L^{τ}, this observable cannot provide further constraints on the RPV couplings. From previous discussions, we show the combined upper bound on $\lambda'_{333}\lambda'^{*}_{333}/m^2_{\tilde{b}_R}$ as a function of $m_{\tilde{b}_R}$ in Fig. 1(d). The upper limit of $\lambda'_{333}\lambda'^{*}_{333}/m^2_{\tilde{b}_R}$ changes around 20% by varying $m_{\tilde{b}_R}$ from 800 GeV to 2000 GeV. Therefore, the allowed parameter space for $m_{\tilde{b}_R} \neq 1$ TeV can approximately be obtained from Fig. 1(a)-1(c) by timing a factor of $(m_{\tilde{b}_R}/1\,\text{TeV})^2$.

4.2 Predictions

In the parameter space allowed by all the constraints at the 2σ level, correlations among several observables are obtained, as shown in Fig. 2. In these figures, the SUSY predictions are central values without theoretical uncertainties. From Fig. 2(a), we can see that the central values of R_D and R_{D^*} are strongly correlated, as expected from Eq. (13). The SUSY effects can only enhance the central value of $R_{D^{(*)}}$ by about 8%, such that the ratios $R_{D^{(*)}}$ approach, but still lie outside, the 2σ range of the HFLAV averages. Therefore, future refined measurements will provide a crucial test to the RPV SUSY explanation of $R_{D^{(*)}}$ anomalies. At Belle II, precisions of $R_{D^{(*)}}$ measurements are expected to be about 2%–4% [71] with a luminosity of 50 ab^{-1}. Fig. 2(b), it can be seen that both R_{D^*} and $\mathcal{B}(B^+ \to K^+\nu\bar{\nu})$ deviate from their SM predictions. The lower bound for the latter is $\mathcal{B}(B^+ \to K^+\nu\bar{\nu}) > 7.37\times$

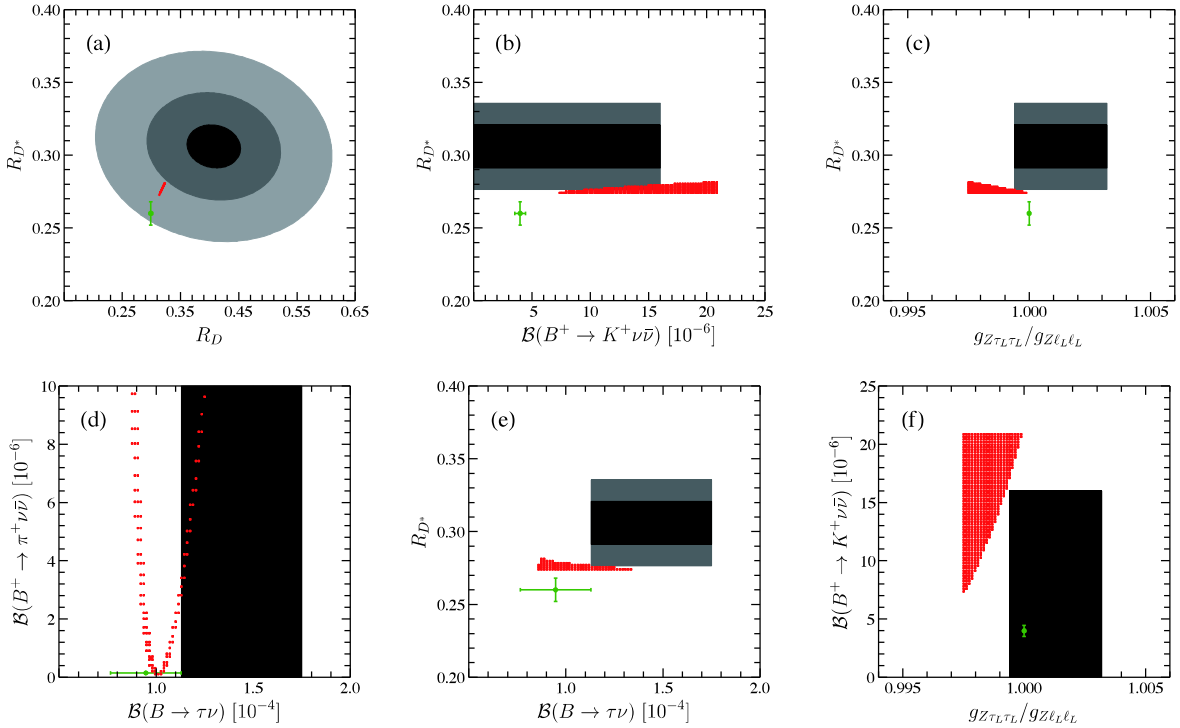

Fig. 2. (color online) Correlations among various observables. SM predictions correspond to the green cross, while the correlations in the RPV SUSY are depicted by red points. In Fig. 2(a), the current HFLAV averages for R_D and R_{D^*} are shown as the black region, and the 2σ (4σ) experimental region is depicted in gray (light gray). In other figures, the 1σ experimental region is shown in black. The 2σ regions for R_{D^*} are also depicted in gray.

10^{-6}, which is due to the lower bound of $\lambda'_{323}\lambda'^{*}_{333} > 0.018$ obtained in the last section. Compared to the SM prediction $\mathcal{B}(B^+ \to K^+\nu\bar{\nu})_{\rm SM} = (3.98 \pm 0.47) \times 10^{-6}$, such significant enhancement makes this decay an important probe of the RPV SUSY effects. In the future, Belle II with $50\,{\rm ab}^{-1}$ data can measure its branching ratio with a precision of 11% [71]. Another interesting correlation arises between $\mathcal{B}(B^+ \to K^+\nu\bar{\nu})$ and $g_{Z\tau_L\tau_L}/g_{Z\ell_L\ell_L}$. As shown in Fig. 2(f), the RPV SUSY effects always enhance $\mathcal{B}(B^+ \to K^+\nu\bar{\nu})$ and suppress $g_{Z\tau_L\tau_L}/g_{Z\ell_L\ell_L}$ simultaneously. When $g_{Z\tau_L\tau_L}/g_{Z\ell_L\ell_L}$ approaches the SM value 1, the branching ratio of $B^+ \to K^+\nu\bar{\nu}$ maximally deviates from its SM prediction. In Fig. 2(d) and 2(e), we show the correlations involving $B \to \tau\nu$ decay. The SUSY prediction on $\mathcal{B}(B \to \tau\bar{\nu})$ is almost in the SM 1σ range. Since the future Belle II sensitivity at $50\,{\rm ab}^{-1}$ is comparable to the current theoretical uncertainties [71], significantly more precise theoretical predictions are required in the future to probe the SUSY effects.

Using the allowed parameter space at the 2σ level derived in the last subsection, we make predictions on the five $b \to c\tau\bar{\nu}$ decays, $B \to D^{(*)}\tau\bar{\nu}$, $B_c \to \eta_c\tau\bar{\nu}$, $B_c \to J/\psi\tau\bar{\nu}$, and $\Lambda_b \to \Lambda_c\tau\bar{\nu}$ decays. In Table 2, the SM and SUSY predictions of the various observables in these decays are presented. The SUSY predictions have included the uncertainties induced by the form factors and CKM matrix elements. At present, there are no available measurements on the $B_c \to \eta_c\tau\bar{\nu}$ and $\Lambda_b \to \Lambda_c\tau\bar{\nu}$ decays. Table 2 shows that, although the SUSY predictions for the branching fractions and the LFU ratios in these two decays overlap with their 1σ SM range, they can be considerably enhanced by the RPV SUSY effects.

Now we start to analyze the q^2 distributions of the differential branching fraction $\mathcal{B}$, LFU ratio R, lepton forward-backward asymmetry $A_{\rm FB}$, polarization fraction of τ lepton P_L^τ, and the polarization fraction of daughter meson ($P_L^{D^*}$, $P_L^{J/\psi}$, $P_L^{\Lambda_c}$). For the two "$B \to P$" transitions $B \to D\tau\bar{\nu}$ and $B_c \to \eta_c\tau\bar{\nu}$, their differential observables in the SM and RPV SUSY are shown in Fig. 3. All the differential distributions of these two decays are very similar, whereas the observables in $B_c \to \eta_c\tau\bar{\nu}$ suffer from larger theoretical uncertainties, which are due to the large uncertainties induced by the $B_c \to \eta_c$ form factors. In the RPV SUSY, the branching fraction of $B \to D\tau\bar{\nu}$ decay can be largely enhanced, while the LFU ratio is almost indistinguishable from the SM prediction. Therefore, it is difficult for the differential distribution of $R_D(q^2)$ to provide testable signature of the RPV SUSY. Moreover, the RPV SUSY does not affect the forward-backward asymmetry $A_{\rm FB}$ and τ polarization fraction P_L^τ in these two decays, as shown in Fig. 3. The reason behind this is that the RPV couplings only modify the Wilson coeffi-

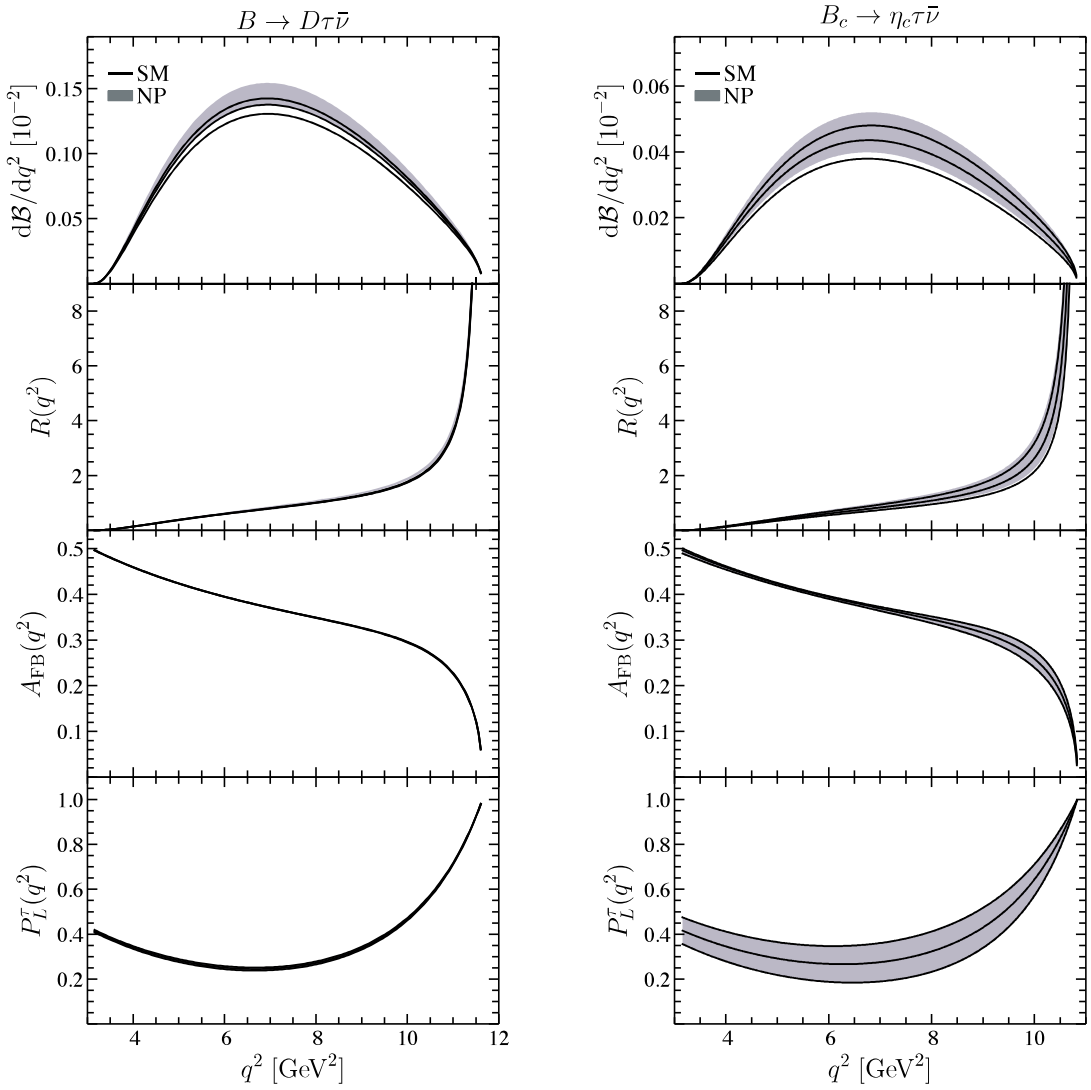

Fig. 3. (color online) Differential observables in $B \to D\tau\bar{\nu}$ (left) and $B_c \to \eta_c\tau\bar{\nu}$ (right) decays. The black curves (gray band) indicate the SM (SUSY) central values with 1σ theoretical uncertainty.

cient $C_{L,2}$, and its effects in the numerator and denominator in Eqs. (11) and (12) cancel out exactly. This feature could be used to distinguish from the NP candidates, which can explain the $R_{D^{(*)}}$ anomaly, but involves scalar or tensor interactions [83, 127, 128].

The differential observables in the $B \to D^*\tau\bar{\nu}$ and $B_c \to J/\psi\tau\bar{\nu}$ decays are shown in Fig. 4. As expected, these two "$B \to V$" processes have very similar distributions. In these two decays, the enhancement by the RPV SUSY effects is not large enough to make the branching ratios deviate from the SM values by more than 1σ. However, the LFU ratios $R_{D^*}(q^2)$ and $R_{J/\psi}(q^2)$ are significantly enhanced in the entire kinematical region, especially in the large dilepton invariant mass region. In this end-point region, the theoretical predictions suffer from very small uncertainties compared to the other kinematical region. By this virtue, the LFU ratios $R_{D^*}(q^2)$ and $R_{J/\psi}(q^2)$ in the RPV SUSY deviate from the SM predictions by about 2σ. Therefore, future measurements on these differential ratios could provide more information about the $R_{D^{(*)}}$ anomaly and are important for the indirect searches for SUSY. In addition, as in the $B \to D\tau\bar{\nu}$ and $B_c \to \eta_c\tau\bar{\nu}$ decays, the angular observables A_{FB}, P_L^τ and $P_L^{D^*,J/\psi}$ are not affected by the SUSY effects.

Figure 5 shows the differential observables in the $\Lambda_b \to \Lambda_c\tau\nu$ decay. The RPV SUSY effects significantly enhance the branching fraction and the LFU ratio. In particular, at the large dilepton invariant mass, the ratio $R_{\Lambda_c}(q^2)$ in the SUSY exhibits a higher than 2σ discrepancy from the SM values. With large Λ_b samples at the future HL-LHC, this decay is expected to provide complementary information to the direct SUSY searches. In addition, as in the other decays, the RPV SUSY effects vanish in various angular observables.

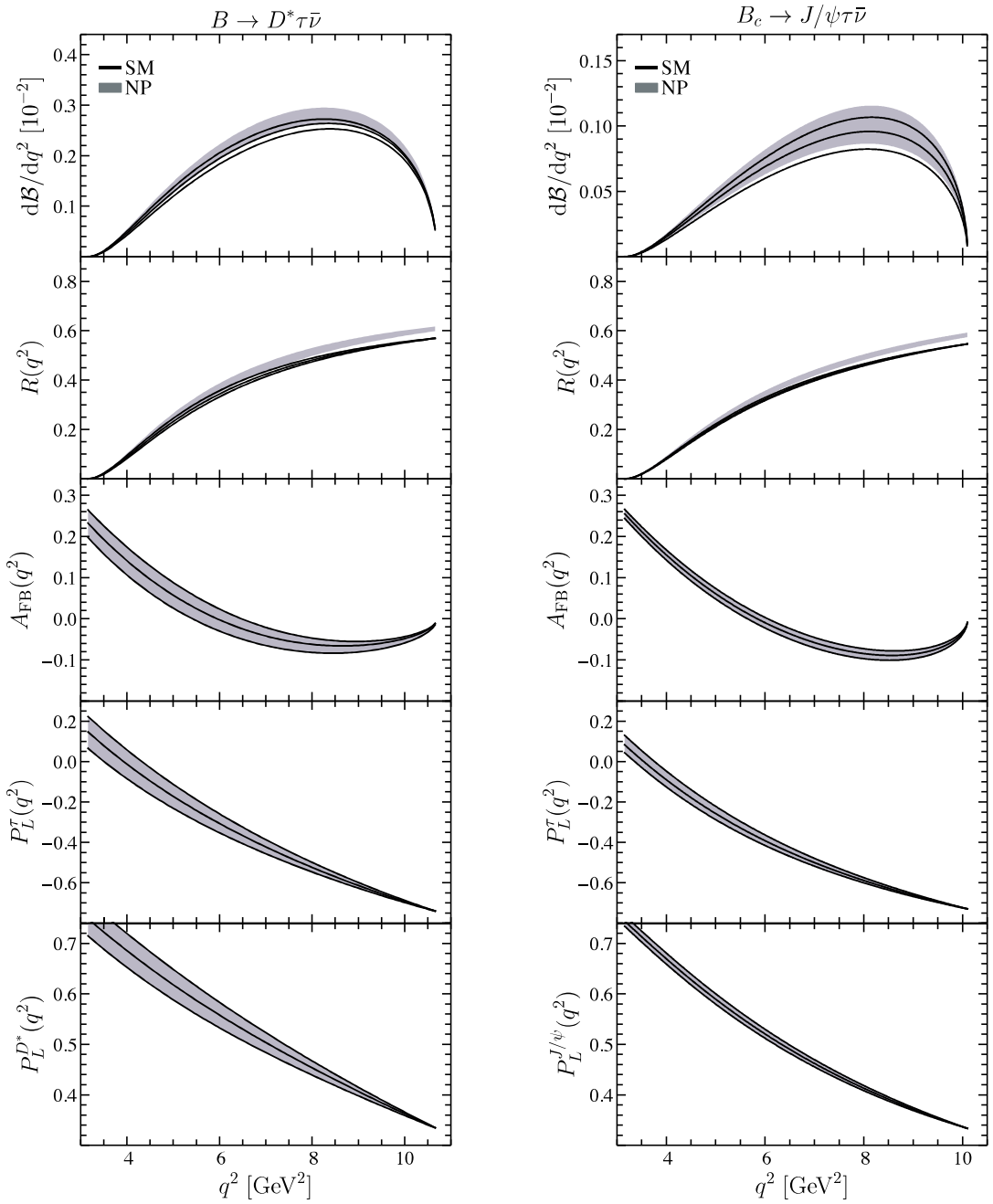

Fig. 4. (color online) Differential observables in $B \to D^*\tau\bar{\nu}$ (left) and $B_c \to J/\psi\tau\bar{\nu}$ (right) decays. The black curves (gray band) indicate the SM (SUSY) central values with 1σ theoretical uncertainty.

5 Conclusions

Recently, several hints of lepton flavor universality violation have been observed in the experimental data of semi-leptonic B decays. Motivated by the recent measurements of $P_L^{D^*}$, we have investigated the RPV SUSY effects in $b \to c\tau\bar{\nu}$ transitions. After considering various flavor processes, we obtain strong constraints of the RPV couplings, which are dominated by $\mathcal{B}(B^+ \to \pi^+\nu\bar{\nu})$, $\mathcal{B}(B^+ \to K^+\nu\bar{\nu})$, and $g_{Z\tau_L\tau_L}$. In the surviving parameter space, the $R_{D^{(*)}}$ anomaly can be explained at the 2σ level, which results in bounds on the coupling products, $-0.082 < \lambda'_{313}\lambda'^*_{333} < 0.087$, $0.018 < \lambda'_{323}\lambda'^*_{333} < 0.057$, and $0.033 < \lambda'_{333}\lambda'^*_{333} < 0.928$. The upper bound on the coupling λ'_{333} prevents this coupling from developing a Landau pole below the GUT scale.

In the parameter space allowed by all the constraints, we make predictions for various flavor processes. For $B^+ \to K^+\nu\bar{\nu}$ decay, a lower bound $\mathcal{B}(B^+ \to K^+\nu\bar{\nu}) > 7.37\times$

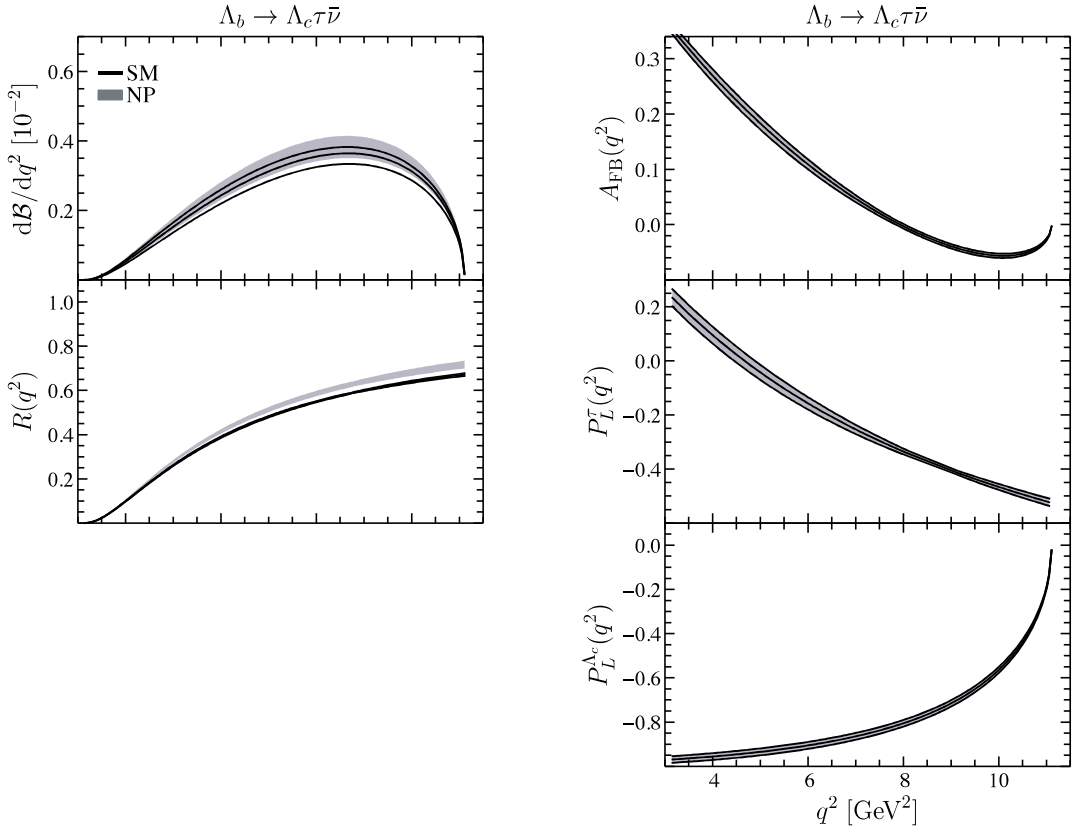

Fig. 5. (color online) Differential observables in $\Lambda_b \to \Lambda_c \tau \bar{\nu}$ decay. Other captions are the same as in Fig. 3.

10^{-6} is obtained. Compared to the SM prediction $(3.98 \pm 0.47) \times 10^{-6}$, this decay can provide an important probe of the RPV SUSY effects at Belle II. We also find interesting correlations among R_D, R_{D^*}, $\mathcal{B}(B^+ \to K^+ \nu\bar{\nu})$, $\mathcal{B}(B \to \tau\nu)$, and $g_{Z\tau_L\tau_L}/g_{Z\ell_L\ell_L}$. For example, the RPV SUSY effects always enhance $\mathcal{B}(B^+ \to K^+ \nu\bar{\nu})$ and suppress $g_{Z\tau_L\tau_L}/g_{Z\ell_L\ell_L}$ simultaneously, which makes one of them largely deviate from its SM value.

Furthermore, we systematically investigated the RPV SUSY effects in five $b \to c\tau\bar{\nu}$ decays, including $B \to D^{(*)}\tau\bar{\nu}$, $B_c \to \eta_c \tau\bar{\nu}$, $B_c \to J/\psi\tau\bar{\nu}$, and $\Lambda_b \to \Lambda_c \tau\bar{\nu}$ decays, while focusing on the q^2 distributions of the branching fractions, the LFU ratios, and various angular observables. The differential ratios $R_{D^*}(q^2)$, $R_{J/\psi}(q^2)$, and $R_{\Lambda_c}(q^2)$ are significantly enhanced by the RPV SUSY effects in the large dilepton invariant mass region. Although the integrated ratios $R_{D^*,J/\psi,\Lambda_c}$ in the SUSY overlap with the 1σ range of the SM values, the differential ratios $R_{D^*,J/\psi,\Lambda_c}(q^2)$ in this kinematical region exhibit a higher than 2σ discrepancy between the SM and SUSY predictions. In addition, the SM and RPV SUSY predictions of various angular observables are indistinguishable, since the RPV SUSY scenario does not generate new operators beyond the ones of SM.

The decays $B^+ \to K^+ \nu\bar{\nu}$ and $B \to \tau\bar{\nu}$, as well as the differential observables in $b \to c\tau\bar{\nu}$ decays, have the potential to shed new light on the $R_{D^{(*)}}$ anomalies and may serve as a test of the RPV SUSY. With the forthcoming SuperKEKB and the future HL-LHC, our results are expected to provide more information on the $b \to c\tau\bar{\nu}$ transitions and could correlate with the direct searches for SUSY in future high-energy colliders.

We thank Jun-Kang He, Quan-Yi Hu, Xin-Qiang Li, Han Yan, Min-Di Zheng, and Xin Zhang for useful discussions.

Appendix A: Form factors

For the operator in Eq. (5), the hadronic matrix elements of $B \to D$ transition can be parameterized in terms of form factors F_+ and F_0 [28, 102]. In the BGL parameterization, they can be written as expressions of a_n^+ and a_n^0 [11],

$$F_+(z) = \frac{1}{P_+(z)\phi_+(z,\mathcal{N})} \sum_{n=0}^{\infty} a_n^+ z^n(w,\mathcal{N}),$$
$$F_0(z) = \frac{1}{P_0(z)\phi_0(z,\mathcal{N})} \sum_{n=0}^{\infty} a_n^0 z^n(w,\mathcal{N}), \quad \text{(A1)}$$

where $z(w,\mathcal{N}) = (\sqrt{1+w}-\sqrt{2\mathcal{N}})/(\sqrt{1+w}+\sqrt{2\mathcal{N}})$, $w = (m_B^2+m_D^2-q^2)/(2m_Bm_D)$, $\mathcal{N} = (1+r)/(2\sqrt{r})$, and $r = m_D/m_B$. Values of the fit parameters are taken from Ref. [11].

For the $B\to D^*$ transition, the relevant form factors are $A_{0,1,2}$ and V. They can be written in terms of the BGL form factors as

$$\begin{aligned}
A_0(q^2) &= \frac{m_B+m_{D^*}}{2\sqrt{m_Bm_{D^*}}}P_1(w),\\
A_1(q^2) &= \frac{f(w)}{m_B+m_{D^*}},\\
A_2(q^2) &= \frac{(m_B+m_{D^*})\left[(m_B^2-m_{D^*}^2-q^2)f(w)-2m_{D^*}\mathcal{F}_1(w)\right]}{\lambda_{D^*}(q^2)},\\
V(q^2) &= m_Bm_{D^*}(m_B+m_{D^*})\frac{\sqrt{w^2-1}}{\sqrt{\lambda_{D^*}(q^2)}}g(w),
\end{aligned} \tag{A2}$$

where $w = (m_B^2+m_{D^*}^2-q^2)/2m_Bm_{D^*}$ and $\lambda_{D^*} = [(m_B-m_{D^*})^2-q^2][(m_B+m_{D^*})^2-q^2]$. The four BGL form factors can be expanded as a series in z

$$\begin{aligned}
f(z) &= \frac{1}{P_{1+}(z)\phi_f(z)}\sum_{n=0}^{\infty}a_n^f z^n,\\
\mathcal{F}_1(z) &= \frac{1}{P_{1+}(z)\phi_{\mathcal{F}_1}(z)}\sum_{n=0}^{\infty}z_n^{\mathcal{F}_1}z^n,\\
g(z) &= \frac{1}{P_{1-}(z)\phi_g(z)}\sum_{n=0}^{\infty}a_n^g z^n,\\
P_1(z) &= \frac{\sqrt{r}}{(1+r)B_{0-}(z)\phi_{P_1}(z)}\sum_{n=0}^{\infty}a_n^{P_1}z^n,
\end{aligned} \tag{A3}$$

where $z = (\sqrt{w+1}-\sqrt{2})/(\sqrt{w+1}+\sqrt{2})$ and $r = m_{D^*}/m_B$. Explicit expressions of the Blaschke factors $P_{1\pm}$ and B_{0-}, and the outer functions $\phi_i(z)$ can be found in Refs. [14, 129]. We also adopt the values of the fit parameters in Refs. [14, 129].

The $\Lambda_b\to\Lambda_c$ hadronic matrix elements can be written in terms of the helicity form factors $F_{0,+,\perp}$ and $G_{0,+,\perp}$ [75, 76]. Following Ref. [75], the lattice calculations are fitted to two Bourrely-Caprini-Lellouch z-parameterization [130]. In the so-called "nominal fit", a form factor has the following form

$$f(q^2) = \frac{1}{1-q^2/(m_{\rm pole}^f)^2}[a_0^f+a_1^f z^f(q^2)], \tag{A4}$$

while the form factor in the "higher-order fit" is given by

$$\begin{aligned}
f_{\rm HO}(q^2) = &\frac{1}{1-q^2/(m_{\rm pole}^f)^2}\left\{a_{0,\rm HO}^f\right.\\
&\left.+a_{1,\rm HO}^f z^f(q^2)+a_{2,\rm HO}^f[z^f(q^2)]^2\right\},
\end{aligned} \tag{A5}$$

where $z^f(q^2) = \left(\sqrt{t_+^f-q^2}-\sqrt{t_+^f-t_0}\right)\Big/\left(\sqrt{t_+^f-q^2}+\sqrt{t_+^f-t_0}\right)$, $t_0 = (m_{\Lambda_b}-m_{\Lambda_c})^2$, and $t_+^f = (m_{\rm pole}^f)^2$. Values of the fit parameters are taken from Ref. [76].

The form factors for $B_c\to J/\psi$ and $B_c\to\eta_c$ transitions are taken from the results in the Covariant Light-Front Approach in Ref. [16].

References

1 J. P. Lees et al (BaBar Collaboration), Phys. Rev. Lett., **109**: 101802 (2012), arXiv:1205.5442
2 J. P. Lees et al (BaBar Collaboration), Phys. Rev. D, **88**(7): 072012 (2013), arXiv:1303.0571
3 M. Huschle et al (Belle Collaboration), Phys. Rev. D, **92**(7): 072014 (2015), arXiv:1507.03233
4 Y. Sato et al (Belle Collaboration), Phys. Rev. D, **94**(7): 072007 (2016), arXiv:1607.07923
5 S. Hirose et al (Belle Collaboration), Phys. Rev. Lett., **118**(21): 211801 (2017), arXiv:1612.00529
6 S. Hirose et al (Belle Collaboration), Phys. Rev. D, **97**(1): 012004 (2018), arXiv:1709.00129
7 R. Aaij et al (LHCb Collaboration), Phys. Rev. Lett., **115**(11): 111803 (2015), arXiv:1506.08614
8 R. Aaij et al (LHCb Collaboration), Phys. Rev. Lett., **120**(17): 171802 (2018), arXiv:1708.08856
9 R. Aaij et al (LHCb Collaboration), Phys. Rev. D, **97**(7): 072013 (2018), arXiv:1711.02505
10 Heavy Flavor Averaging Group Collaboration, Y. Amhis et al., Eur. Phys. J. C, **77**: 895 (2017), arXiv: 1612.07233. updated results and plots available at https://hflav.web.cern.ch
11 D. Bigi and P. Gambino, Phys. Rev. D, **94**(9): 094008 (2016), arXiv:1606.08030
12 S. Jaiswal, S. Nandi, and S. K. Patra, JHEP, **12**: 060 (2017), arXiv:1707.09977
13 F. U. Bernlochner, Z. Ligeti, M. Papucci et al, Phys. Rev. D, **95**(11): 115008 (2017), arXiv:1703.05330
14 D. Bigi, P. Gambino, and S. Schacht, JHEP, **11**: 061 (2017), arXiv:1707.09509
15 R. Aaij et al (LHCb Collaboration), Phys. Rev. Lett., **120**(12): 121801 (2018), arXiv:1711.05623
16 W. Wang, Y.-L. Shen, and C.-D. Lu, Phys. Rev. D, **79**: 054012 (2009), arXiv:0811.3748
17 R. Aaij et al (LHCb Collaboration), Phys. Rev. Lett., **113**: 151601 (2014), arXiv:1406.6482
18 R. Aaij et al (LHCb Collaboration), JHEP, **08**: 055 (2017), arXiv:1705.05802
19 G. Hiller and F. Kruger, Phys. Rev. D, **69**: 074020 (2004), arXiv:hep-ph/0310219
20 M. Bordone, G. Isidori, and A. Pattori, Eur. Phys. J. C, **76**(8): 440 (2016), arXiv:1605.07633
21 Y. Sakaki, M. Tanaka, A. Tayduganov et al, Phys. Rev. D, **91**(11): 114028 (2015), arXiv:1412.3761
22 B. Bhattacharya, A. Datta, D. London et al, Phys. Lett. B, **742**: 370-374 (2015), arXiv:1412.7164
23 L. Calibbi, A. Crivellin, and T. Ota, Phys. Rev. Lett., **115**: 181801 (2015), arXiv:1506.02661
24 R. Alonso, B. Grinstein, and J. Martin Camalich, JHEP, **10**: 184 (2015), arXiv:1505.05164
25 R. Alonso, A. Kobach, and J. Martin Camalich, Phys. Rev. D, **94**(9): 094021 (2016), arXiv:1602.07671
26 F. Feruglio, P. Paradisi, and A. Pattori, Phys. Rev. Lett., **118**(1): 011801 (2017), arXiv:1606.00524
27 Z. Ligeti, M. Papucci, and D. J. Robinson, JHEP, **01**: 083 (2017), arXiv:1610.02045
28 D. Bardhan, P. Byakti, and D. Ghosh, JHEP, **01**: 125 (2017), arXiv:1610.03038
29 R. Dutta and A. Bhol, Phys. Rev. D, **96**(3): 036012 (2017), arXiv:1611.00231
30 S. Bhattacharya, S. Nandi, and S. K. Patra, Phys. Rev. D, **95**(7): 075012 (2017), arXiv:1611.04605
31 M. Bordone, G. Isidori, and S. Trifinopoulos, Phys. Rev. D, **96**(1): 015038 (2017), arXiv:1702.07238
32 D. Choudhury, A. Kundu, R. Mandal et al, Phys. Rev. Lett.,

119(15): 151801 (2017), arXiv:1706.08437
33 S. Bhattacharya, S. Nandi, and S. Kumar Patra, arXiv: 1805.08222
34 Q.-Y. Hu, X.-Q. Li, and Y.-D. Yang, arXiv: 1810.04939
35 Y. Sakaki and H. Tanaka, Phys. Rev. D, **87**(5): 054002 (2013), arXiv:1205.4908
36 A. Crivellin, C. Greub, and A. Kokulu, Phys. Rev. D, **86**: 054014 (2012), arXiv:1206.2634
37 Y.-Y. Fan, Z.-J. Xiao, R.-M. Wang et al, arXiv: 1505.07169
38 C. S. Kim, Y. W. Yoon, and X.-B. Yuan, JHEP, **12**: 038 (2015), arXiv:1509.00491
39 I. Doršner, S. Fajfer, A. Greljo et al, Phys. Rept., **641**: 1-68 (2016), arXiv:1603.04993
40 B. Dumont, K. Nishiwaki, and R. Watanabe, Phys. Rev. D, **94**(3): 034001 (2016), arXiv:1603.05248
41 G. Hiller, D. Loose, and K. Schönwald, JHEP, **12**: 027 (2016), arXiv:1609.08895
42 D. A. Faroughy, A. Greljo, and J. F. Kamenik, Phys. Lett. B, **764**: 126-134 (2017), arXiv:1609.07138
43 B. Bhattacharya, A. Datta, J.-P. Guévin et al, JHEP, **01**: 015 (2017), arXiv:1609.09078
44 L. Wang, J. M. Yang, and Y. Zhang, Nucl. Phys. B, **924**: 47-62 (2017), arXiv:1610.05681
45 O. Popov and G. A. White, Nucl. Phys. B, **923**: 324-338 (2017), arXiv:1611.04566
46 A. Celis, M. Jung, X.-Q. Li et al, Phys. Lett. B, **771**: 168-179 (2017), arXiv:1612.07757
47 M. Wei and Y. Chong-Xing, Phys. Rev. D, **95**(3): 035040 (2017), arXiv:1702.01255
48 G. Cvetič, F. Halzen, C. S. Kim et al, Chin. Phys. C, **41**(11): 113102 (2017), arXiv:1702.04335
49 P. Ko, Y. Omura, Y. Shigekami et al, Phys. Rev. D, **95**(11): 115040 (2017), arXiv:1702.08666
50 C.-H. Chen and T. Nomura, Eur. Phys. J. C, **77**(9): 631 (2017), arXiv:1703.03646
51 A. Crivellin, D. Müller, and T. Ota, JHEP, **09**: 040 (2017), arXiv:1703.09226
52 Y. Cai, J. Gargalionis, M. A. Schmidt et al, JHEP, **10**: 047 (2017), arXiv:1704.05849
53 S. Iguro and K. Tobe, Nucl. Phys. B, **925**: 560-606 (2017), arXiv:1708.06176
54 L. Di Luzio, A. Greljo, and M. Nardecchia, Phys. Rev. D, **96**(11): 115011 (2017), arXiv:1708.08450
55 L. Calibbi, A. Crivellin, and T. Li, Phys. Rev. D, **98**(11): 115002 (2018), arXiv:1709.00692
56 X.-G. He and G. Valencia, Phys. Lett. B, **779**: 52-57 (2018), arXiv:1711.09525
57 K. Fuyuto, H.-L. Li, and J.-H. Yu, Phys. Rev. D, **97**(11): 115003 (2018), arXiv:1712.06736
58 S.-P. Li, X.-Q. Li, Y.-D. Yang et al, JHEP, **09**: 149 (2018), arXiv:1807.08530
59 A. Angelescu, D. Bečirević, D. A. Faroughy et al, JHEP, **10**: 183 (2018), arXiv:1808.08179
60 T. J. Kim, P. Ko, J. Li et al, arXiv: 1812.08484
61 Y. Li and C.-D. Lü, Sci. Bull., **63**: 267-269 (2018), arXiv:1808.02990
62 S. Bifani, S. Descotes-Genon, A. Romero Vidal et al, J. Phys. G, **46**(2): 023001 (2019), arXiv:1809.06229
63 K. Adamczyk (Belle, Belle II Collaboration), *Semitauonic B decays at Belle/Belle II, in 10th International Workshop on the CKM Unitarity Triangle (CKM 2018) Heidelberg, Germany, September 17-21, 2018*, 2019. arXiv: 1901.06380
64 A. Abdesselam et al (Belle Collaboration), *Measurement of the D^* polarization in the decay $B_0 \to D^* \tau + \nu_\tau$*, in *10th International Workshop on the CKM Unitarity Triangle (CKM 2018) Heidelberg, Germany, September 17-21, 2018*, 2019. arXiv: 1903.03102
65 A. K. Alok, D. Kumar, S. Kumbhakar et al, Phys. Rev. D, **95**(11): 115038 (2017), arXiv:1606.03164
66 M. Tanaka and R. Watanabe, Phys. Rev. D, **82**: 034027 (2010), arXiv:1005.4306
67 M. Tanaka and R. Watanabe, Phys. Rev. D, **87**(3): 034028 (2013), arXiv:1212.1878
68 Z.-R. Huang, Y. Li, C.-D. Lu et al, Phys. Rev. D, **98**(9): 095018 (2018), arXiv:1808.03565
69 S. Iguro, T. Kitahara, Y. Omura et al, JHEP, **02**: 194 (2019), arXiv:1811.08899
70 P. Asadi, M. R. Buckley, and D. Shih, Phys. Rev. D, **99**(3): 035015 (2019), arXiv:1810.06597
71 W. Altmannshofer et al (Belle II Collaboration), *The Belle II Physics Book*, arXiv: 10.1808.10567
72 N. G. Deshpande and A. Menon, JHEP, **01**: 025 (2013), arXiv:1208.4134
73 N. G. Deshpande and X.-G. He, Eur. Phys. J. C, **77**(2): 134 (2017), arXiv:1608.04817
74 W. Altmannshofer, P. Bhupal Dev, and A. Soni, Phys. Rev. D, **96**(9): 095010 (2017), arXiv:1704.06659
75 W. Detmold, C. Lehner, and S. Meinel, Phys. Rev. D, **92**(3): 034503 (2015), arXiv:1503.01421
76 A. Datta, S. Kamali, S. Meinel et al, JHEP, **08**: 131 (2017), arXiv:1702.02243
77 R. Barbier et al, Phys. Rept., **420**: 1-202 (2005), arXiv:hep-ph/0406039
78 M. Chemtob, Prog. Part. Nucl. Phys., **54**: 71-191 (2005), arXiv:hep-ph/0406029
79 J. Zhu, H.-M. Gan, R.-M. Wang et al, Phys. Rev. D, **93**(9): 094023 (2016), arXiv:1602.06491
80 J. Zhu, B. Wei, J.-H. Sheng et al, Nucl. Phys. B, **934**: 380-395 (2018), arXiv:1801.00917
81 C. Brust, A. Katz, S. Lawrence et al, JHEP, **03**: 103 (2012), arXiv:1110.6670
82 M. Papucci, J. T. Ruderman, and A. Weiler, JHEP, **09**: 035 (2012), arXiv:1110.6926
83 M. Bauer and M. Neubert, Phys. Rev. Lett., **116**(14): 141802 (2016), arXiv:1511.01900
84 A. Celis, M. Jung, X.-Q. Li et al, JHEP, **01**: 054 (2013), arXiv:1210.8443
85 J. A. Bailey et al, Phys. Rev. Lett., **109**: 071802 (2012), arXiv:1206.4992
86 D. Bečirević, N. Košnik, and A. Tayduganov, Phys. Lett. B, **716**: 208-213 (2012), arXiv:1206.4977
87 C. W. Murphy and A. Soni, Phys. Rev. D, **98**(9): 094026 (2018), arXiv:1808.05932
88 P. Colangelo and F. De Fazio, Phys. Rev. D, **61**: 034012 (2000), arXiv:hep-ph/9909423
89 V. V. Kiselev, arXiv: hep-ph/0211021
90 E. Hernandez, J. Nieves, and J. M. Verde-Velasco, Phys. Rev. D, **74**: 074008 (2006), arXiv:hep-ph/0607150
91 M. A. Ivanov, J. G. Korner, and P. Santorelli, Phys. Rev. D, **73**: 054024 (2006), arXiv:hep-ph/0602050
92 C.-F. Qiao and R.-L. Zhu, Phys. Rev. D, **87**(1): 014009 (2013), arXiv:1208.5916
93 W.-F. Wang, Y.-Y. Fan, and Z.-J. Xiao, Chin. Phys. C, **37**: 093102 (2013), arXiv:1212.5903
94 Y. K. Hsiao and C. Q. Geng, Chin. Phys. C, **41**(1): 013101 (2017), arXiv:1607.02718
95 R. Watanabe, Phys. Lett. B, **776**: 5-9 (2018), arXiv:1709.08644
96 C.-T. Tran, M. A. Ivanov, J. G. Körner et al, Phys. Rev. D, **97**(5): 054014 (2018), arXiv:1801.06927
97 T. Gutsche, M. A. Ivanov, J. G. Körner et al, Phys. Rev. D, **91**(7): 074001 (2015), arXiv:1502.04864
98 S. Shivashankara, W. Wu, and A. Datta, Phys. Rev. D, **91**(11): 115003 (2015), arXiv:1502.07230
99 R. Dutta, Phys. Rev. D, **93**(5): 054003 (2016), arXiv:1512.04034
100 R. N. Faustov and V. O. Galkin, Phys. Rev. D, **94**(7): 073008 (2016), arXiv:1609.00199
101 K. Hagiwara, A. D. Martin, and M. F. Wade, Nucl. Phys. B,

327: 569-594 (1989)
102 Y. Sakaki, M. Tanaka, A. Tayduganov et al, Phys. Rev. D, **88**(9): 094012 (2013), arXiv:1309.0301
103 Y.-M. Wang, Y.-B. Wei, Y.-L. Shen et al, JHEP, **06**: 062 (2017), arXiv:1701.06810
104 B. Grinstein and A. Kobach, Phys. Lett. B, **771**: 359-364 (2017), arXiv:1703.08170
105 N. Gubernari, A. Kokulu, and D. van Dyk, JHEP, **01**: 150 (2019), arXiv:1811.00983
106 A. Berns and H. Lamm, JHEP, **12**: 114 (2018), arXiv:1808.07360
107 W. Wang and R. Zhu, arXiv: 1808.10830
108 F. U. Bernlochner, Z. Ligeti, and D. J. Robinson, arXiv: 1902.09553
109 D. Leljak, B. Melic, and M. Patra, arXiv: 1901.08368
110 S. Aoki et al (Flavour Lattice Averaging Group Collaboration), *FLAG Review 2019*, arXiv: 1902.08191
111 I. Caprini, L. Lellouch, and M. Neubert, Nucl. Phys. B, **530**: 153-181 (1998), arXiv:hep-ph/9712417
112 M. Neubert, Z. Ligeti, and Y. Nir, Phys. Lett. B, **301**: 101-107 (1993), arXiv:hep-ph/9209271
113 M. Neubert, Z. Ligeti, and Y. Nir, Phys. Rev. D, **47**: 5060-5066 (1993), arXiv:hep-ph/9212266
114 Z. Ligeti, Y. Nir, and M. Neubert, Phys. Rev. D, **49**: 1302-1309 (1994), arXiv:hep-ph/9305304
115 C. G. Boyd, B. Grinstein, and R. F. Lebed, Phys. Rev. D, **56**: 6895-6911 (1997), arXiv:hep-ph/9705252
116 A. J. Buras, J. Girrbach-Noe, C. Niehoff et al, JHEP, **02**: 184 (2015), arXiv:1409.4557
117 F. Feruglio, P. Paradisi, and A. Pattori, JHEP, **09**: 061 (2017), arXiv:1705.00929
118 SLD Electroweak Group, DELPHI, ALEPH, SLD, SLD Heavy Flavour Group, OPAL, LEP Electroweak Working Group, L3 Collaboration, S. Schael et al, Phys. Rept., **427**: 257-454 (2006), arXiv:hep-ex/0509008
119 X.-Q. Li, Y.-D. Yang, and X. Zhang, JHEP, **08**: 054 (2016), arXiv:1605.09308
120 R. Alonso, B. Grinstein, and J. Martin Camalich, Phys. Rev. Lett., **118**(8): 081802 (2017), arXiv:1611.06676
121 A. M. Sirunyan et al (CMS Collaboration), Eur. Phys. J. C, **78**(9): 707 (2018), arXiv:1803.02864
122 M. Tanabashi et al (Particle Data Group Collaboration), Phys. Rev. D, **98**(3): 030001 (2018)
123 J. Charles, A. Hocker, H. Lacker et al (CKMfitter Group Collaboration), Eur. Phys. J. C, **41**(1): 1-131 (2005), arXiv:hep-ph/0406184
124 M. Jung, X.-Q. Li, and A. Pich, JHEP, **10**: 063 (2012), arXiv:1208.1251
125 C.-W. Chiang, X.-G. He, F. Ye et al, Phys. Rev. D, **96**(3): 035032 (2017), arXiv:1703.06289
126 V. D. Barger, M. S. Berger, R. J. N. Phillips et al, Phys. Rev. D, **53**: 6407-6415 (1996), arXiv:hep-ph/9511473
127 M. Freytsis, Z. Ligeti, and J. T. Ruderman, Phys. Rev. D, **92**(5): 054018 (2015), arXiv:1506.08896
128 X.-Q. Li, Y.-D. Yang, and X. Zhang, JHEP, **02**: 068 (2017), arXiv:1611.01635
129 D. Bigi, P. Gambino, and S. Schacht, Phys. Lett. B, **769**: 441-445 (2017), arXiv:1703.06124
130 C. Bourrely, I. Caprini, and L. Lellouch, Phys. Rev. D, **79**: 013008 (2009), arXiv:0807.2722